Water Oxidation

DOI: 10.1002/anie.201102648

Effects of a Proximal Base on Water Oxidation and Proton Reduction Catalyzed by Geometric Isomers of $[Ru(tpy)(pynap)(OH_2)]^{2+}$**

Julie L. Boyer, Dmitry E. Polyansky, David J. Szalda, Ruifa Zong, Randolph P. Thummel, and Etsuko Fujita**

The importance of pendent bases in promoting proton-coupled electron-transfer (PCET) reactions with low activation barriers has been discussed for H^+ reduction or H_2 oxidation in MeCN.[1] PCET is also essential for the four-electron oxidation of water in order to mitigate charge buildup and to reduce overpotential.[2] Designing molecular catalysts that facilitate these multielectron and multiproton processes has proven to be a formidable challenge.[3] Ruthenium polypyridyl compounds have received considerable attention as water oxidation catalysts. Dinuclear ruthenium species have been studied for some time,[4] while only recently mononuclear ruthenium species were reported as effective water oxidation catalysts.[5–8] In nature, water oxidation is performed at the manganese-containing oxygen-evolving complex (OEC), and electron transfer is coupled to proton movement by precisely positioned proton relays in the nearby protein scaffold.[2,9]

We have previously demonstrated the utility of ruthenium polypyridyl complexes with pendent bases to act as water oxidation catalysts with the compounds $[Ru(L)(4\text{-}R\text{-}pyridine)_2(OH_2)]^{2+}$ ($R = CF_3$, CH_3, NMe_2; L = 4-*tert*-butyl-2,6-di([1′,8′]-naphthyrid-2′-yl)pyridine).[5] To further examine the role that pendent bases play in the oxidation and reduction of ruthenium polypyridyl complexes, we have isolated the compounds p-$[Ru(tpy)(pynap)(OH_2)]^{2+}$ (p = proximal, tpy = 2,2′;6′,2″-terpyridine, pynap = 2-(pyrid-2′-yl)-1,8-naphthyridine), $\mathbf{1}(OH_2)^{2+}$ and d-$[Ru(tpy)(pynap)(OH_2)]^{2+}$ (d = distal), $\mathbf{2}(OH_2)^{2+}$, which differ in the orientation of the asymmetric pynap ligand (Scheme 1 and Figure 1). Herein we present the complexes' redox and spectroscopic properties and report the intriguing catalytic activity for the oxidation of H_2O and the reduction of protons. While $\mathbf{1}(OH_2)^{2+}$ shows catalytic activity toward proton reduction but not toward water oxidation, the geometric isomer $\mathbf{2}(OH_2)^{2+}$ exhibits the opposite behavior.

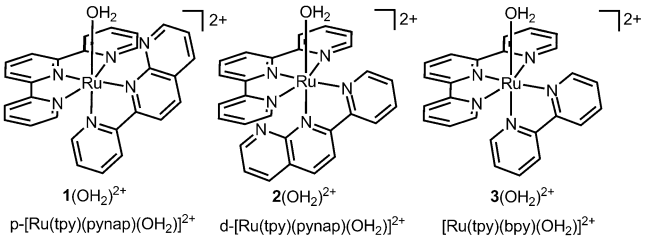

Scheme 1. Structures of complexes.

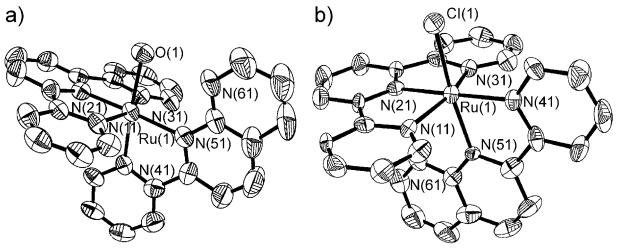

Figure 1. The molecular structures of cations in a) $[\mathbf{1}(OH_2)]Cl_2$ and b) $[\mathbf{2}(Cl)](PF_6)_2$.

The ^1H NMR spectra of the geometric isomers support the proposed orientations of the pynap ligand (Figures S1 and S2 in the Supporting Information). The single-crystal X-ray structures of $[\mathbf{1}(OH_2)]Cl_2$ and the electrochemically oxidized Ru^{III} species $[\mathbf{2}(Cl)](PF_6)_2$ were determined (see Tables S1–S3 in the Supporting Information).[10] They further confirmed the orientation of the asymmetric pynap ligand (Figure 1). A spectrophotometric acid–base titration was performed with each of the isomers. The UV/Vis spectra remained unchanged at low pH values, thus indicating that the uncoordinated naphthyridyl nitrogen atom is not protonated, even under strongly acidic conditions (pH 0). At high pH values, the aqua ligand was deprotonated: $\mathbf{2}(OH_2)^{2+}$ displayed a lower pK_a than the reported value for $\mathbf{3}(OH_2)^{2+}$ (9.1 vs. 9.7),[11] owing to the increased electronegativity of pynap versus bpy. A pK_a of 11.3 was observed for $\mathbf{1}(OH_2)^{2+}$ owing to a hydrogen-bonding interaction between the uncoordinated naphthyridyl nitrogen atom and the aqua ligand.

[*] Dr. J. L. Boyer, Dr. D. E. Polyansky, Dr. D. J. Szalda, Dr. E. Fujita
Chemistry Department, Brookhaven National Laboratory
Upton, NY 11973-5000 (USA)
E-mail: fujita@bnl.gov
Dr. R. Zong, Prof. R. P. Thummel
Department of Chemistry, University of Houston
Houston, TX 77204-5003 (USA)
E-mail: thummel@uh.edu
Dr. D. J. Szalda
Department of Natural Science
Baruch College, New York, NY 10010 (USA)

[**] We thank Dr. James T. Muckerman for valuable discussions. The work at Brookhaven National Laboratory (BNL) is funded under contract DE-AC02-98CH10886 and the work at Houston is funded under contract DE-FG02-07ER15888 with the U.S. Department of Energy and supported by its Division of Chemical Sciences, Geosciences, & Biosciences, Office of Basic Energy Sciences. The BNL authors also thank the U.S Department of Energy for funding under the BES Hydrogen Fuel Initiative. R.Z. and R.P.T. also thank the Robert A. Welch Foundation (E-621). tpy = 2,2′;6′,2″-terpyridine, pynap = 2-(pyrid-2′-yl)-1,8-naphthyridine.

Supporting information for this article is available on the WWW under http://dx.doi.org/10.1002/anie.201102648.

Table 1: Physical data for compounds containing pynap and bpy co-ligands in MeCN.

Compound	λ_{max} [nm]	$E_{1/2}$ [V][b] ($Ru^{III/II}$)	$E_{1/2}$ [V][b] ($L/L^{\bullet-}$)	Ref.
$[Ru(bpy)_3]^{2+}$	450	1.24	−1.34, −1.52, −1.75	[12]
$[Ru(pynap)_3]^{2+}$	526	1.08	−0.99, −1.23, −1.53	[12]
$\mathbf{2}(Cl)^{+}$	568	0.76	−1.13, −1.49 (ir)	[7]
$\mathbf{3}(Cl)^{+}$	508	0.80	−1.44, −1.59	[7]
$\mathbf{1}(OH_2)^{2+}$[a]	532	1.11	−0.87, −1.34 (ir)	[c]
$\mathbf{2}(OH_2)^{2+}$[a]	534	1.06	−1.01, −1.35 (ir)	[c]
$\mathbf{3}(OH_2)^{2+}$[a]	474	1.12	−1.23, −1.45 (ir)	[c]
$\mathbf{1}(NCMe)^{2+}$	492	1.28	−1.01, −1.45 (ir)	[c]
$\mathbf{2}(NCMe)^{2+}$	498	1.27	−1.00, −1.45 (ir)	[c]
$\mathbf{3}(NCMe)^{2+}$	455	1.29	−1.27, −1.54 (ir)	[13]

[a] Acetone was used for measurements of aqua complexes. [b] Potentials measured with a Ag/AgCl electrode were converted to values vs. the saturated calomel electrode (SCE), ir = quasi-irreversible or irreversible. [c] This work.

The absorption and electrochemical data for Ru complexes containing either bpy or pynap ligands in non-aqueous media are summarized in Table 1. Relative to complexes containing bpy ligands, analogues with the pynap ligand display a metal-to-ligand charge-transfer (MLCT) band at lower energies, a lower oxidation potential for the $Ru^{II/III}$ couple, and a lower reduction potential for the ligand-based reduction couple. A comparison of the electrochemical data for the two geometric isomers $\mathbf{1}(OH_2)^{2+}$ and $\mathbf{2}(OH_2)^{2+}$ revealed a more positive reduction potential for the pynap/pynap$^{\bullet-}$ process in the isomer with the proximal base (−0.87 V vs. −1.01 V), whereas the two isomers $\mathbf{1}(NCMe)^{2+}$ and $\mathbf{2}(NCMe)^{2+}$ display similar reduction potentials for the pynap$^{\bullet-}$/pynap process (−1.01 V vs. −1.00 V). This finding provided further evidence of an interaction between the aqua ligand and the pendent base in the complex $\mathbf{1}(OH_2)^{2+}$.

Cyclic and square-wave voltammograms were recorded in aqueous solutions at varying acid concentrations for both geometric isomers (Figures S3 and S4 in the Supporting Information). The plot of $E_{1/2}$ versus pH value (Pourbaix diagram, Figure 2) for the complex $\mathbf{2}(OH_2)^{2+}$ displayed a similar topology and pK_a values as the Pourbaix diagram of $[Ru(tpy)(bpy)(OH_2)]^{2+}$ ($\mathbf{3}(OH_2)^{2+}$).[10] A comparison of the Pourbaix diagrams of the geometric isomers revealed the unique aqueous redox chemistry of $\mathbf{1}(OH_2)^{2+}$. The first oxidation process in $\mathbf{2}(OH_2)^{2+}$ exhibits pH-independent regions (pH 0–1.5 and pH 9.1–11.4) and is $1e^-$ in nature below pH 11.4. However, the first oxidation process in $\mathbf{1}(OH_2)^{2+}$ is $2e^-$ and proton-coupled through the pH range 1.5–13. Between pH 1.5 and 4, the voltammogram of $\mathbf{1}(OH_2)^{2+}$ displays two oxidation events ($[Ru^{II}(OH_2)]^{2+}/[Ru^{IV}(OH)]^{3+}$ and $[Ru^{IV}(OH)]^{3+}/[Ru^{V}O]^{3+}$) with slopes of −30 mV per pH unit and −59 mV per pH unit, thus indicating that they are $2e^-/1H^+$ and $1e^-/1H^+$ processes, respectively (Figure S3 in the Supporting Information). Below pH 1.5, it seems that the first process becomes pH-independent ($[Ru^{II}(OH_2)]^{2+}/[Ru^{IV}(OH_2)]^{4+}$), and the second one is $2e^-/2H^+$ ($[Ru^{IV}(OH_2)]^{4+}/[Ru^{VI}O]^{4+}$). While the first oxidation potentials between pH 1.5 and 4 could be fit with a slope of −59 mV per pH unit, such an assignment cannot explain the oxidation events at higher potentials. The $2e^-$ nature of the first oxidation process in the compound $\mathbf{1}(OH_2)^{2+}$ was further confirmed by coulometry and cerium titration experiments. Between pH 4 and 11, the oxidation potential of $\mathbf{1}(OH_2)^{2+}$ displays a slope of −59 mV per pH unit, corresponding to a $2e^-/2H^+$ transformation ($[Ru^{II}(OH_2)]^{2+}/[Ru^{IV}O]^{2+}$).

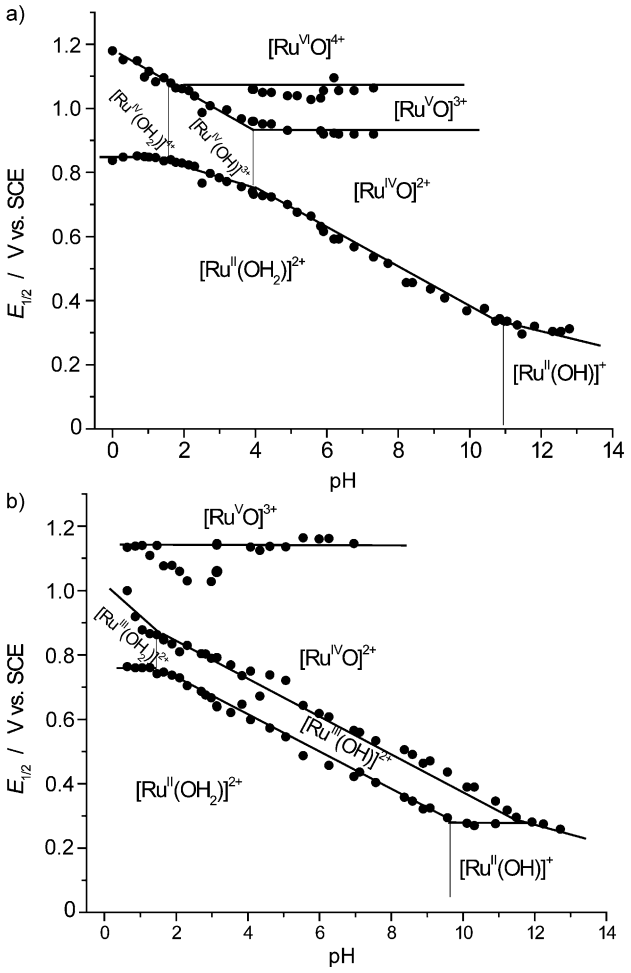

Figure 2. Pourbaix diagram of geometric isomers a) $\mathbf{1}(OH_2)^{2+}$ and b) $\mathbf{2}(OH_2)^{2+}$.

The very weak signals around 1.1 V with slope 50 mV per pH unit observed for **2** in the range pH 1–3 are likely due to a small contamination by complex $\mathbf{1}(OH_2)^{2+}$, since $\mathbf{2}(OH_2)^{2+}$ slowly converts to $\mathbf{1}(OH_2)^{2+}$ under ambient fluorescent light. Also, we tentatively assigned weak signals around 1.1 V observed in the range of pH 3–8 as the $Ru^{V}{=}O/Ru^{IV}{=}O$ couple of $\mathbf{2}(OH_2)^{2+}$; however, we cannot exclude the contamination problem.

After the second redox process ($[Ru^{IV}(OH_2)]^{2+}/[Ru^{VI}O]^{4+}$) at pH 1, the cathodic scan displays a new feature at 500 mV versus SCE (Figure S5 in the Supporting Information). The intensity of the signal at 500 mV increases as the initial potential is increased (1180 to 1360 mV) or the time the electrode is held at the positive potential before the scan is increased (2 to 20 s). This increase in intensity is likely due to the formation of an oxidation

product of $\mathbf{1}(OH_2)^{2+}$, possibly the $[Ru^{III}(OOH)]^{2+}$ species based on our voltammetry data (Figure S5 in the Supporting Information) and the assignment of intermediates in related systems.[8j]

The isomer $\mathbf{1}(OH_2)^{2+}$ undergoes a $2e^-$ and a $2e^-/2H^+$ process at pH 1 to form a highly oxidized $[Ru^{IV}(OH_2)]^{4+}$ and $[Ru^{VI}O]^{4+}$ species, respectively, at a low applied potential (below 1.2 V vs. SCE; Figure 2). The first oxidation process for the isomer $\mathbf{1}(OH_2)^{2+}$ was examined using the chemical oxidant $(NH_4)_2[Ce(NO_3)_6]$ (CAN) in 0.1M HNO_3. Upon addition of up to two equivalents of CAN, the peaks in the UV/Vis absorption spectrum at 526 and 314 nm decreased in intensity (Figures S6 and S7 in the Supporting Information). Isosbestic points were observed at 412 and 333 nm, thus confirming the concerted nature of this $2e^-$ oxidation process that is chemically reversible. Reduction of the newly formed solution with two equivalents of Fe^{II} led to recovery of 96% of the starting complex $\mathbf{1}(OH_2)^{2+}$.

The catalytic currents of $\mathbf{1}(OH_2)^{2+}$ and $\mathbf{2}(OH_2)^{2+}$ are shown in Figure 3. The activity for water oxidation was studied with an excess of the sacrificial oxidant CAN (Figure 4). The oxygen evolved was detected with an Ocean Optics O_2 probe. The isomer $\mathbf{1}(OH_2)^{2+}$ proved to be a poor water oxidation catalyst, with a turnover number (TON) of approximately one and an initial rate of $1.1\times10^{-3}\,s^{-1}$ (defined as TON s^{-1}) for O_2 evolution. When the headspace of the oxidized solution of $\mathbf{1}^{2+}$ was analyzed by mass spectrometry, both CO_2 and O_2 were detected. When an additional aliquot of CAN was injected into the oxidized solution of $\mathbf{1}^{2+}$, no additional CO_2 or O_2 was detected (Figure S8 in the Supporting Information).

The compound $\mathbf{2}(OH_2)^{2+}$ displayed remarkable activity for water oxidation. The compound $\mathbf{2}(OH_2)^{2+}$ displays a TON of over 3200 with the initial rate $1.8\times10^{-2}\,s^{-1}$ for O_2 evolution. Previously, a TON of 1170 in 20 h was reported for the compound $[\mathbf{2}(Cl)]PF_6$ in the presence of trace organic solvent.[7] In separate runs, we found that the catalytic activity of $\mathbf{2}(OH_2)^{2+}$ was suppressed by the addition of 10 equiv NaCl or trace amounts of MeCN. We re-examined $[\mathbf{2}(Cl)]PF_6$ in strictly aqueous media and observed a TON of 2700 in 48 h. The compounds $\mathbf{3}(OH_2)^{2+}$ and $[Ru(tpy)(biq)(OH_2)](PF_6)_2$ (biq = 2,2′-biquinoline) were also evaluated as water oxidation catalysts. They displayed TON values of 460 and 2, respectively. The isomer $\mathbf{1}(OH_2)^{2+}$ reaches the highly oxidized Ru^{VI} state at a low potential, but it performed poorly as a water oxidation catalyst when CAN was used. The low turnover number might be due to catalyst decomposition, which was evident from the carbon dioxide detected during catalysis runs (Figure S8 in the Supporting Information). The isomer $\mathbf{2}(OH_2)^{2+}$, however, proved to be a much better water oxidation catalyst than the recently heavily investigated $\mathbf{3}(OH_2)^{2+}$.[8c,d,e,h] While we observed a relatively slow aquation of $\mathbf{2}(Cl)^+$ at neutral pH, it has been suggested that the Cl ligand might remain in the coordination sphere, leading to a seven-coordinate ruthenium oxo species in the higher oxidation states.[7] In fact, we isolated crystals of the Cl-bound Ru^{III} complex $[\mathbf{2}(Cl)](PF_6)_2$ by slow evaporation of the resultant pale green solution from the bulk electrolysis of $[\mathbf{2}(Cl)]PF_6$ (at 0.86 V vs. SCE) under an argon flow (see Figure 1b).

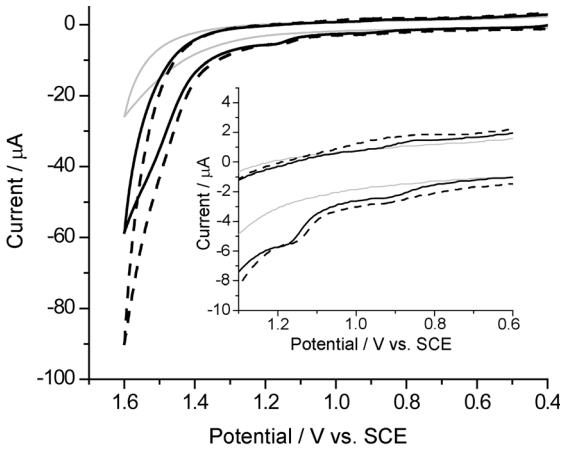

Figure 3. Cyclic voltammogram of $\mathbf{1}(OH_2)^{2+}$ (solid), $\mathbf{2}(OH_2)^{2+}$ (dashed), and baseline (gray) at pH 1. Inset: Expanded version showing cyclic voltammogram below 1.3 V.

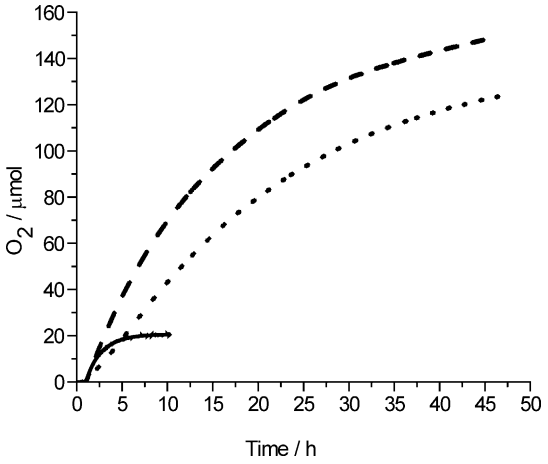

Figure 4. Plots of detected O_2 versus time for $\mathbf{2}(OH_2)^{2+}$ (dashed), $\mathbf{2}(Cl)^+$ (dotted), and $\mathbf{3}(OH_2)^{2+}$ (solid). O_2 formation for $\mathbf{1}(OH_2)^{2+}$ is not shown because of the small TON.

We further explored catalytic properties of $\mathbf{1}(OH_2)^{2+}$ and $\mathbf{2}(OH_2)^{2+}$ towards proton reduction. The Pourbaix diagram for $\mathbf{1}(OH_2)^{2+}$ (Figure 5a) clearly indicates that below pH 8, the reduction of the complex is accompanied by protonation to form $[Ru(tpy)(pynap{\cdot}H)(OH_2)]^{2+}$. The geometric isomers were evaluated electrochemically as H_2 production catalysts in MeCN. While solutions of $\mathbf{1}(NCMe)^{2+}$ displayed catalytic currents for proton reduction upon the addition of a weak acid such as acetic acid ($pK_a = 22.5$M; Figure 5b), those of $\mathbf{2}(NCMe)^{2+}$ did not show significantly enhanced current (Figure S9 in the Supporting Information). These preliminary results clearly demonstrate the utility of appropriately positioned proton relays.

It is very intriguing that the ruthenium species with a proximal base ($\mathbf{1}(OH_2)^{2+}$), with a proton relay in the vicinity of the coordinated ligand to induce PCET reactions, is not a good catalyst for water oxidation with CAN as a sacrificial oxidant. However, many ruthenium polypyridyl complexes with pendent bases, including $[Ru(L)(4'\text{-R-pyridine})_2$-

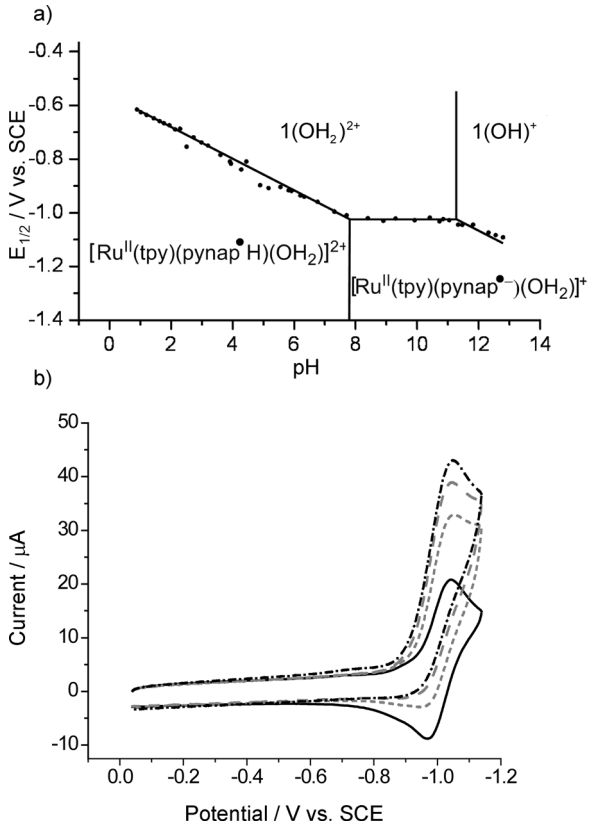

Figure 5. a) Reduction part of Pourbaix diagram for $\mathbf{1}(OH_2)^{2+}$. b) Catalytic currents observed by the addition of HOAc (1 (dotted gray line), 2 (dashed gray line), and 3 mM (dot-dashed black line)) to 1 mM solution of $\mathbf{1}(NCMe)^{2+}$ (solid line) in 0.1 N Bu_4NPF_6 MeCN with scan rates of 100 $mV\,s^{-1}$.

$(OH_2)]^{2+}$ (R = CF_3, CH_3, NMe_2; L = 4-*tert*-butyl-2,6-di([1′,8′]-naphthyrid-2′-yl)pyridine) and related complexes act as water oxidation catalysts with CAN.[5,6] Does a strong oxidant like CAN produce the highly reactive Ru^{VI} species that may decompose very quickly by oxidizing its own pynap or tpy ligand? Can the catalyst catalyze water oxidation at neutral pH? We are currently investigating electrochemical water oxidation by applying controlled potentials. We are also exploring mechanisms and kinetics of proton reduction catalyzed by $\mathbf{1}(OH_2)^{2+}$ to understand the detailed role of the pendent base.

Experimental Section

The synthesis of $[Ru(tpy)(pynap)(OH_2)](PF_6)_2$ is slightly modified from literature procedures.[7] The ligand pynap,[14] $[Ru(tpy)Cl_3]$,[15] and $[Ru(tpy)(biq)(OH_2)](PF_6)_2$[16] were prepared according to literature procedures. The reaction of $[Ru(tpy)Cl_3]$ with pynap in the presence of NEt_3 under reflux conditions produced a mixture of compounds $\mathbf{1}(OH_2)^{2+}$ and $\mathbf{2}(Cl)^{+}$ in a ratio $\mathbf{2}(Cl)^{+}/\mathbf{1}(OH_2)^{2+}$ of 1:1. The compounds $\mathbf{1}(OH_2)^{2+}$ and $\mathbf{2}(Cl)^{+}$ were separated by column chromatography (on alumina, acetone eluent). Treatment of $[\mathbf{2}(Cl)]^{+}$ with a silver salt afforded the compound $\mathbf{2}(OH_2)^{2+}$. UV/Vis spectra were measured on a Hewlett–Packard 8452A diode array spectrophotometer and a Cary 500 Scan UV/Vis/NIR spectrophotometer. The ^1H NMR spectra were acquired on a Bruker UltraShield 400 MHz instrument. Electrospray ionization-mass spectra (ESI-MS) were acquired with a Thermo Finnigan mass spectrometer. Elemental analyses were conducted by Robertson Microlit Laboratories. Square-wave and cyclic voltammograms were obtained using a BAS100 electrochemical system. Oxygen measurements were performed using a calibrated O_2 probe (Ocean Optics probe with a factory multipoint calibration). A single-point reset was performed before each catalysis run. The detailed experimental conditions for all experiments, including preparation of complexes, spectroscopic measurements, electrochemical measurements, O_2 evolution, and X-ray single crystal diffraction studies are shown in the Supporting Information.

Note added in revision: A similar communication by Yagi et al.[17] was published during the revision of this manuscript.

Received: April 17, 2011
Revised: September 19, 2011
Published online: November 4, 2011

Keywords: electron transfer · isomers · proton reduction · ruthenium · water oxidation

[1] a) M. R. DuBois, D. L. DuBois, *Chem. Soc. Rev.* **2009**, *38*, 62–72; b) M. R. DuBois, D. L. DuBois, *Acc. Chem. Res.* **2009**, *42*, 1974–1982, and references therein.
[2] M. H. Huynh, T. J. Meyer, *Chem. Rev.* **2007**, *107*, 5004–5064, and references therein.
[3] a) Forum on Making Oxygen, *Inorg. Chem.* **2008**, *47*, 1697–1861; b) H. Dau, C. Limberg, T. Reier, M. Risch, S. Roggan, P. Strasser, *ChemCatChem* **2010**, *2*, 724–761; c) H. Yamazaki, A. Shouji, M. Kajita, M. Yagi, *Coord. Chem. Rev.* **2010**, *254*, 2483–2491; d) M. Yagi, M. Kaneko, *Chem. Rev.* **2000**, *100*, 21–36, and references therein.
[4] a) S. W. Gersten, G. J. Samuels, T. J. Meyer, *J. Am. Chem. Soc.* **1982**, *104*, 4029–4030; b) C. Sens, I. Romero, M. Rodriguez, A. Llobet, T. Parella, J. Benet-Buchholz, *J. Am. Chem. Soc.* **2004**, *126*, 7798–7799; c) J. K. Hurst, *Coord. Chem. Rev.* **2005**, *249*, 313–328; d) J. J. Concepcion, J. W. Jurss, M. K. Brennaman, P. G. Hoertz, A. O. T. Patrocinio, N. Y. M. Iha, J. L. Templeton, T. J. Meyer, *Acc. Chem. Res.* **2009**, *42*, 1954–1965; e) T. Wada, K. Tsuge, K. Tanaka, *Inorg. Chem.* **2001**, *40*, 329–337; f) J. T. Muckerman, D. E. Polyansky, T. Wada, K. Tanaka, E. Fujita, *Inorg. Chem.* **2008**, *47*, 1787–1802; g) F. Bozoglian, S. Romain, M. Z. Ertem, T. K. Todorova, C. Sens, J. Mola, M. Rodriguez, I. Romero, J. Benet-Buchholz, X. Fontrodona, C. J. Cramer, L. Gagliardi, A. Llobet, *J. Am. Chem. Soc.* **2009**, *131*, 15176–15187; h) Y. H. Xu, L. L. Duan, L. P. Tong, B. Akermark, L. C. Sun, *Chem. Commun.* **2010**, *46*, 6506–6508; i) L. Francàs, X. Sala, E. Escudero-Adán, J. Benet-Buchholz, L. Escriche, A. Llobet, *Inorg. Chem.* **2011**, *50*, 2771–2781.
[5] R. Zong, R. P. Thummel, *J. Am. Chem. Soc.* **2005**, *127*, 12802–12803.
[6] Z. Deng, H. W. Tseng, R. Zong, D. Wang, R. P. Thummel, *Inorg. Chem.* **2008**, *47*, 1835–1848.
[7] H. W. Tseng, R. Zong, J. T. Muckerman, R. Thummel, *Inorg. Chem.* **2008**, *47*, 11763–11773.
[8] a) J. J. Concepcion, J. W. Jurss, J. L. Templeton, T. J. Meyer, *J. Am. Chem. Soc.* **2008**, *130*, 16462–16463; b) L. Duan, A. Fischer, Y. Xu, L. Sun, *J. Am. Chem. Soc.* **2009**, *131*, 10397–10399; c) S. Masaoka, K. Sakai, *Chem. Lett.* **2009**, *38*, 182–183; d) D. J. Wasylenko, C. Ganesamoorthy, M. A. Henderson, B. D. Koivisto, H. D. Osthoff, C. P. Berlinguette, *J. Am. Chem. Soc.* **2010**, *132*, 16094–16106; e) D. J. Wasylenko, C. Ganesamoorthy, M. A. Henderson, C. P. Berlinguette, *Inorg. Chem.* **2011**, *50*, 3662–3672; f) Z. Chen, J. J. Concepcion, H. Luo, J. F. Hull, A. Paul, T. J. Meyer, *J. Am. Chem. Soc.* **2010**, *132*, 17670–17673;

g) X. Sala, M. Z. Ertem, L. Vigara, T. K. Todorova, W. Z. Chen, R. C. Rocha, F. Aquilante, C. J. Cramer, L. Gagliardi, A. Llobet, *Angew. Chem.* **2010**, *122*, 7911 – 7913; *Angew. Chem. Int. Ed.* **2010**, *49*, 7745 – 7747; h) M. Yoshida, S. Masaoka, J. Abe, K. Sakai, *Chem. Asian J.* **2010**, *5*, 2369 – 2378; i) L. L. Duan, Y. H. Xu, L. P. Tong, L. C. Sun, *ChemSusChem* **2011**, *4*, 238 – 244; j) J. J. Concepcion, M.-K. Tsai, J. T. Muckerman, T. J. Meyer, *J. Am. Chem. Soc.* **2010**, *132*, 1545 – 1557; k) M. Yagi, S. Tajima, M. Komia, H. Yamazaki, *Dalton Trans.* **2011**, *40*, 3802 – 3804; l) L. Duan, Y. H. Xu, M. Gorlov, L. P. Tong, S. Andersson, L. C. Sun, *Chem. Eur. J.* **2010**, *16*, 4659 – 4668.

[9] a) J. P. McEvoy, G. W. Brudvig, *Phys. Chem. Chem. Phys.* **2004**, *6*, 4754 – 4763; b) H. J. Hwang, P. Dilbeck, R. J. Debus, R. L. Burnap, *Biochemistry* **2007**, *46*, 11987 – 11997; c) T. J. Meyer, M. H. V. Huynh, H. H. Thorp, *Angew. Chem.* **2007**, *119*, 5378 – 5399; *Angew. Chem. Int. Ed.* **2007**, *46*, 5284 – 5304.

[10] CCDC 821728 and 821729 contain the supplementary crystallographic data for this paper. These data can be obtained free of charge from The Cambridge Crystallographic Data Centre via www.ccdc.cam.ac.uk/data_request/cif.

[11] K. J. Takeuchi, M. S. Thompson, D. W. Pipes, T. J. Meyer, *Inorg. Chem.* **1984**, *23*, 1845 – 1851.

[12] E. B. Amira-Soriaga, S. D. Sprouse, R. J. Watts, W. C. Kaska, *Inorg. Chim. Acta* **1984**, *84*, 135 – 139.

[13] S. C. Rasmussen, S. E. Ronco, D. A. Mlsna, A. M. A. Billadeau, W. T. Pennington, J. W. Kolis, J. D. Petersen, *Inorg. Chem.* **1995**, *34*, 821 – 829.

[14] C. S. Campos-Fernández, L. M. Thomson, J. R. Galán-Mascarós, X. Ouyang, K. R. Dunbar, *Inorg. Chem.* **2002**, *41*, 1523 – 1533.

[15] R. A. Leising, S. A. Kubow, M. R. Churchill, L. A. Buttrey, J. W. Ziller, K. J. Takeuchi, *Inorg. Chem.* **1990**, *29*, 1306 – 1312.

[16] C. A. Bessel, J. A. Margarucci, J. H. Acquaye, R. S. Rubino, J. Crandall, A. J. Jircitano, K. J. Takeuchi, *Inorg. Chem.* **1993**, *32*, 5779 – 5784.

[17] H. Yamazaki, T. Hakamata, M. Komi, M. Yagi, *J. Am. Chem. Soc.* **2011**, *133*, 8846 – 8849

